Theoretical Studies on Excited States of Biorelated Systems from Gas Phase to Aqueous Solution

Junfeng Li, Xugeng Guo, Yuan Zhao, and Zexing Cao*

Excited-state properties of molecules play a pivotal role in understanding their photophysical and photochemical behaviors. With the fast development of computational methodologies, the low-lying states of biorelated systems have been extensively investigated theoretically. Here, we review our recent works on the excited states of selected nucleobases and their related systems in the gas and condensed phases. The simulated electronic spectra of coumarin reproduce the band shape of experimental spectra and provide a basis to reasonably assign the observed bands. The absorption spectra and the excited-state dynamics of nucleic acid bases and their analogs in the gas phase and in aqueous solution have been explored by the combined quantum mechanics and molecular mechanics (QM/MM) calculations and QM/MM-based dynamics simulations with surface hopping. Based on extensive calculations and dynamics simulations, the solvent effects on the excited states and their dynamical behaviors have been discussed. © 2015 Wiley Periodicals, Inc.

DOI: 10.1002/qua.24879

Introduction

Sunlight is the energy source for almost all life on the earth, but exposure to the strong sunlight too much can be harmful. The nucleic acid bases, as the fundamental building blocks of life, may undergo extremely ultrafast nonradiative decay in vacuum, solution, and DNA environments, which dissipate the excess energy to the surroundings in the form of heat. Such remarkable photodynamical properties play a crucial role in DNA photostability. Generally, molecules harvest visible and ultraviolet lights and are initially populated the singlet excited states. The excited-state molecule is less stable and it may evolve to the ground state through photophysical and photochemical processes.

The electronic spectra, including absorption, fluorescence, phosphorescence, and so forth, may present important information for the electronic structure change and they can be used to explore the excited-state process of molecules. As most of photobiological molecules usually exist in solution or in the protein environment, the band shapes of their observed electronic spectra are usually broad and structureless owing to strong influence of the polarity of solvent and the doppler effect. Consequently, a lot of important information about the early dynamics of molecules is concealed under the diffuse electronic spectra.[1] Alternatively, the simulation of vibronic spectra of molecule makes the exploration of these information become possible.

Recently, a series of computational tools for the vibronic spectrum simulation of medium-size molecules in the gas and condensed phases have been developed.[2–8] Lots of experimental electronic spectra have been interpreted reasonably based on the simulated vibronic spectra.[9–14] A recent study of vibronic fluorescence spectra of coumarin has been presented and selected vibronic bands of spectra have been interpreted and assigned.[15]

Besides the radiative decay, the nonradiative decay is its most important competitive channel. The internal conversion IC may dominate the relaxation of the excited-state molecule to the ground state during the nonradiative decay.[16] After molecule is populated to an excited state, it may have chance to reach the conical intersection region,[17] where there is complete breakdown of Born–Oppenheimer approximation. In the conical intersection, the potential energy surfaces (PESs) of different electronic states become degenerate with specific molecular geometries. The conical intersection provides ultrafast path for the nonradiative deactivation of molecule, and plays a critical role in photophysics and photochemistry. The radiationless decay of pterin[18] and PCN2NM[19] in their excited states has been discussed based on extensive electronic structural calculations.

The photodynamics provides more direct information about the dynamical behaviors of excited-state molecules.[20] Theoretically, the excited-state dynamics simulations have been also motivated by the development of experimental femtosecond spectroscopic techniques.[21] Based on the hybrid QM/MM simulations with surface hopping, the excited-state dynamics of several biorelated systems has been investigated, and our dynamical simulations reveal remarkable structural and solvent effects on their nonradiative deactivation behaviors.[22,23]

J. Li, X. Guo, Y. Zhao, Zexing Cao
State Key Laboratory of Physical Chemistry of Solid Surfaces and Fujian Provincial Key Lab of Theoretical and Computational Chemistry, College of Chemistry and Chemical Engineering, Xiamen University, Xiamen 361005, People's Republic of China
E-mail: zxcao@xmu.edu.cn

Contract grant sponsor: National Science Foundation of China (NSFC); contract grant number: 21133007, 21373164.
Contract grant sponsor: Ministry of Science and Technology; contract grant numbers: 2011CB808504, 2012CB214900.

Junfeng Li received a M.S. in Chemistry from Henan University in 2009. He is currently a Ph.D. student in theoretical chemistry at Xiamen University under the supervision of Zexing Cao. His research interests include vibronic spectra and excited states properties of biomolecules.

Xugeng Guo received his Ph.D. in Theoretical Chemistry from Xiamen University with Zexing Cao in 2014. He now works in Henan University. His research interests include the excited state and photochemistry, especially the ultrafast nonadiabatic decay of nucleic acid bases and their analogs.

Yuan Zhao received a M.S. in Chemistry from Henan University in 2012. She is currently a Ph.D. student in theoretical chemistry at Xiamen University under the supervision of Zexing Cao. Her current research interests include QM/MM simulations on the enzymatic catalysis and excited states properties of biomolecules.

Zexing Cao received his Ph.D. from Sichuan University with Guosen Yan in 1993. From 1999 to 2000, he worked as a Postdoctoral Fellow with Prof. M.B. Hall at Texas A&M University. From 2000 to 2001, he spent an AvH Fellow year with Prof. S.D. Peyerimhoff at Bonn University. In 2001, he became Professor at Xiamen University. His research interests cover excited state and photochemistry, theoretical catalysis, modeling enzymatic catalysis, and computational materials.

As most photophysical and photochemical processes occur in solution or in complex environments, the structures and relative energies of excited states may be changed to some extent, compared to the gas-phase situation. Accordingly, the reliable theoretical treatment should cover the solvent effect. The hybrid QM/MM methods show good balance between computational ability and costs, and can be used to deal with the environmental effect on excited states of biorelated systems. To have insight into the hydrogen bond network around the excited-state bases, the absorption spectra of nucleic acid bases in aqueous solution have been studied by the combined QM/MM and cluster-continuum computational protocol.

In the following, we will give a brief introduction to computational methods for excited states and their dynamics at first, and then selected results about the stimulated vibronic spectra, excited states, and ultrafast nonadiabatic decay of biorelated systems will be presented and discussed.

Computation Methods

Ab initio electronic structure calculations

Nowadays, many *ab initio* quantum chemistry methods have been used to calculate the properties of excited states. The single-reference methods, including the second-order approximate coupled-cluster (CC2),[24] the algebraic diagrammatic construction,[25] and the equation of motion coupled cluster (EOM-CC),[26] and so forth, are relatively cheap and reliable for most vertical excitation energies of low-lying states with the single-reference character. For the structure search of excited state and conical intersection, the multireference and multiconfiguration methods are required. In particular, the multiconfigurational self consistent field,[27] the multireference configuration interaction (MRCI),[28,29] and the complete active second-order perturbation theory (CASPT2) methods[30] can be used to calculate the analytical gradient of the ground and excited states.[31–33] The analytical nonadiabatic coupling can also be

calculated by complete active space multiconfiguration self-consistent field (CASSCF) and MRCI methods.[34] It was well known that the dynamic electron correlation effect, which is important for the relative energies of excited states, is not considered by the CASSCF method, and the multireference second-order perturbation theory and MRCI have been widely used to improve the CASSCF-predicted relative energies of excited states.

The time-dependent density functional theory (TD-DFT) is an alternative choice to the study of excited-state properties. Besides the linear response TD-DFT method,[35] the restricted open-shell Kohn–Sham,[36] restricted ensemble-reference Kohn–Sham[37] time-dependent density functional tight-binding[38] methods can also be used for the calculation of vertical transition energies. The TD-DFT methodology can be used to determine the analytical gradient of energy and nonadiabatic coupling vector of excited states.[39,40] Generally, B3LYP[41] and PBE0[42] functions are popular for the calculation of properties of the ground and excited states. However, TD-DFT usually fails to describe the multireference and charge transfer states[43] and it also cannot be used to evaluate the PES surrounding the conical intersection because of the linear response approximation and its single-reference feature.

Simulations of vibronic spectra

As we are interested in the strong absorption and emission bands of electronic spectra, the Franck–Condon approximation has been considered here. The simulation of the vibronic spectra is based on the reliable quantum-chemically molecular parameters, including the geometries, vibrational frequencies, normal modes, relative energies, transition dipole moments of the ground and excited states, and so on.[44] Temperature effect has been taken into account by considering the Boltzmann distribution of the vibrational states of the initial electronic state.[45] The normal coordinates of initial state and final state are related by the linear transformation of the Duschinsky matrix.[46] Stick spectra have been obtained through calculation of Franck–Condon factor of molecule, which can be expanded to convolution spectrum by Gaussian or Lorentzian broadenings and compared with experimental spectrum band.

Ab initio-based excited-state dynamics

In recent years, nonadiabatic dynamics simulations become popular in searching the reaction paths and conical intersections in photophysical and photochemical processes. Many different theoretical techniques such as multiple spawning,[47] Liouville dynamics,[48] and independent trajectories[49] have been developed for the nonadiabatic dynamics simulation. The surface hopping method, which is a kind of trajectory-based approaches, has been widely used owing to its simplicity, practicality, and affordable computational costs.[50] In the surface hopping dynamics simulations, a trajectory has a hopping probability from one state to the other state near the conical intersection region. The fewest-switches-surface-hopping algorithm is used to evaluate if the transition occurs. For a decay process of excited state, the hopping points define the range where the internal conversion takes place.

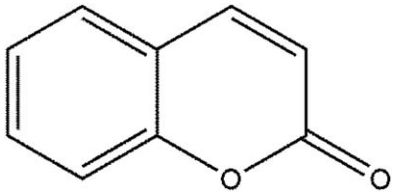

Figure 1. The schematic representation of coumarin.

Hybrid QM/MM method

This hybrid QM/MM strategy was introduced by Warshel and Levitt[51] and has been extensively applied to study of chemical processes in solution and proteins.[52] The central idea of QM/MM is that a large molecule system can be divided into two parts: the QM region and the MM region. In QM/MM calculation of excited states in biorelated systems, the QM region, usually the chromophore in solution or protein, has been described by *ab initio* quantum mechanics, while the MM part, the solution or the complex environment surrounding the QM part, is treated with the molecular mechanical force field. Here, the QM region was dealt with the CASSCF method while the water molecules were described by the TIP3P model,[53] which allow us to explore the excited states of nucleobase analogs and their PESs in solution. The QM/MM simulations with surface hopping are also used to explore the excited-state dynamics of the biorelated systems.

Results and Discussion

Vibronic emission spectra of coumarin

Coumarin is the basic structural unit of the benzopyrone family of functional compounds, and it is usually involved in laser dyes,[54] perfume,[55] and medicine.[56] To rationalize spectroscopic features of these heterocyclic oxygen compounds, we performed a thorough investigation on the excited-state properties and vibronic coupling interactions in absorption and emission spectra of coumarin (Fig. 1).[15]

At 12 k, the emission spectra of coumarin in polar solutions have been reported and rich vibronic structures including two vibronic peaks and a shoulder peak have been observed.[57] Based on the predicted structures and frequencies of S_1 and S_0 in coumarin calculated at the B3LYP/6–31G(d) level of theory, the $S_0 \leftarrow S_1$ vibronic fluorescence spectrum has been simulated and shown in Figure 2. We note that the simulated fluorescence spectra of coumarin in the gas phase, cyclohexane, and water by the B3LYP method do not reproduce the experimental bands very well.[57]

Considering the multireference character of the S_1 state, the CASSCF approach has been used for the geometry optimization and frequency calculations of the low-lying states of coumarin, and these CASSCF-optimized structures and corresponding frequencies have been used in simulation of the vibronic fluorescence spectrum. As Figure 3 shows, the computed spectrum shows good agreement with the experimental data and important spectral features are reproduced reasonably. Both computational and experimental bands

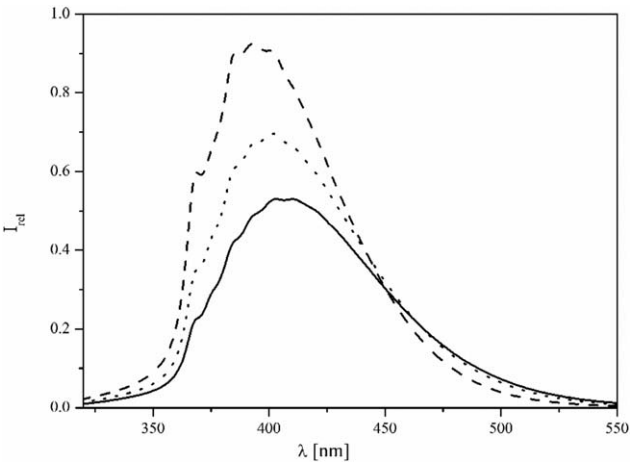

Figure 2. Simulated Franck–Condon $S_0 \leftarrow S_1$ fluorescence spectrum of coumarin in gas (dash line), cyclohexane (point line), water (solid line) by B3LYP.

exhibit the two-peak structure, and a gap of 20 nm between two peaks can be found. All of those important normal modes are relative to the stretching of the C—O bond. These single mode transitions and their combination transitions lead to the maxima of the fluorescence band.

Deactivation pathway of excited states of pterin and PCN2NM

Pterin. Pterin (Fig. 4) and their derivatives, which usually be used as inhibitors,[58] coenzymes,[59] and pigments,[60] are important heterocyclic compounds in biological systems. The concentration of pterin (PT) in body fluids is a critical indication for the clinical diagnosis.[61] We explored the excited-state properties and related photophysical processes of the acidic form of pterin, and plausible radiation and nonradiative deactivation pathways of its singlet excited states have been demonstrated based on extensive calculations.[18]

Table 1 shows the vertical excitation energies and oscillator strengths of the acidic form of pterin determined by CASSCF/CASPT2 caluculations in the gas phase. The calculations show that two strong absorptions observed in experiment arise from the optically bright $^1(\pi\pi^*L_a)$ and $^1(\pi\pi^*L_b)$ states, while the

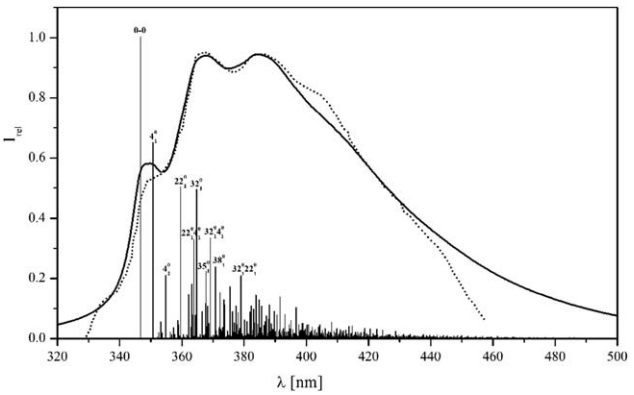

Figure 3. Simulated Franck–Condon $S_0 \leftarrow S_1$ fluorescence spectrum of coumarin by CASSCF (solid line) and the experimental spectrum (point line).

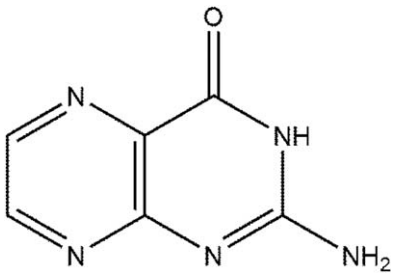

Figure 4. The schematic representation of pterin.

$n \rightarrow \pi^*$ electronic excitations are less accessible. The $^1(n\pi^*)$ state is usually important for the nonradiative decay process, although it is difficult to be observed experimentally. To understand the deactivation mechanisms of the excited singlet states of pterin, the relative energy profiles of the $^1(\pi\pi^*L_a)$ and $^1(n_N\pi^*)$ states have been given in Figure 5. We note that the $^1(n_N\pi^*)$ state can be reached through the internal conversion via the $^1(\pi\pi^*L_a/n_N\pi^*)_{CI}$ conical intersection.

The predicted fluorescence maximum from the $^1(\pi\pi^*L_a)$ state based on its optimized structure is about 3.14 eV in the gas phase, which agrees with the observed emission peak at 439.5 nm (2.82 eV).[62] An interesting experimental finding is that the fluorescence spectra of PT maintain unchanged, regardless of the excitation wavelength in the range of 230–350 nm.[62] This suggests that the $^1(\pi\pi^*L_a)$ state exclusively is responsible for the emission under high-energy irradiation, and the IC processes from high-energy excited states to the $^1(\pi\pi^*L_a)$ state should be easily accessible in the excited state of pterin.

The fluorescence intensity of PT was found to decrease as the excitation energy increases, suggesting that the radiationless decay channel was activated under excess energy. The CASPT2 relative energies of $^1(\pi\pi^*L_a)_{min}$, the saddle point (SP), and $(S_1/S_0)_{CI}$ have been given in Figure 6. The IC decay from $^1(\pi\pi^*L_a)_{min}$ to the ground state via $(S_1/S_0)_{CI}$ is unfavorable thermodynamically and there is a SP separating the $^1(\pi\pi^*)_{min}$ and $(S_1/S_0)_{CI}$ on the PES of S_1. These results can explain the experimental observations that the excited PT is in favor of fluorescence emission, whereas the corresponding decay efficiency becomes slow under the low energy light. Once the excess energy available, the IC process via $(S_1/S_0)_{CI}$ with an out-of-plane distorted geometry will become important for fluorescence loss of PT.

Table 1. CASPT2-predicted vertical transition and emission energies (ΔE in eV) of low-lying singlet excited states of PT in acidic form.

	Vertical transition energies			Vertical emission energies		
State	ΔE	f	Exp.[a]	ΔE	τ (ns)	Exp.[a]
$^1(\pi^*L_a)$	3.984	0.1783	3.65	3.14	2.66	2.82
$^1(n_N\pi^*)$	4.015	0.0066		3.36	0.26	
$^1(n_o\pi^*)$	4.714	0.0016		3.42	4.25	
$^1(\pi\pi^*L_b)$	5.800	0.1423	4.59			

[a] See Ref. [62].

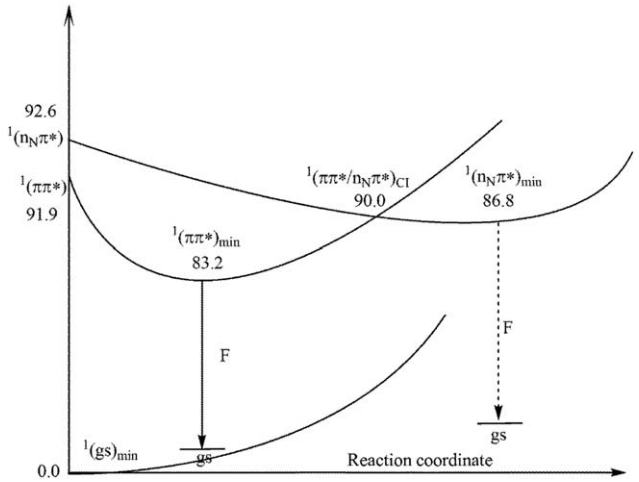

Figure 5. Relative CASPT2 energy profiles for the low-lying states of the excited pterin.

PCN2NM. In past several years, the mechanism for the dual fluorescence phenomenon in charge-transfer molecules has attracted considerable attention.[63] For example, PCN2NM (Fig. 7) without the conjugated bridge between the electronic donor and acceptor moieties has been found to have typical dual fluorescence emissions with a strong peak at 533 nm and a weak band of 290 nm in acetonitrile.[64] We have investigated the nature of the dual fluorescence emission and possible radiation/radiationless decay channels of the excited PCN2NM.[19]

Based on the CASSCF/CASPT2 calculations, the vertical excitation energies, oscillator strengths, and dipole moments of PCN2NM have been shown in Table 2. It can be seen that the oscillator strength for the $^1(\pi\pi^*L_a)$ state is 0.2776, while those of the lower-energy $^1(\pi\pi^*L_b)$ and $^1(n_N\pi^*)$ states are 0.0042 and 0.0276, respectively. This means that the $^1(\pi\pi^*L_a)$ state is easily accessible and should be responsible for the main photophysical processes of PCN2NM will start from the excited $^1(\pi\pi^*L_a)$ state. CASPT2 calculations also predicts that the $^1(n_N\pi^*)$ states have larger dipole moments than the ground state, and they could be characterized as the CT state, denoted as $^1(S_1\text{-CT})$ for the low-energy $^1(n_N\pi^*)$. The $^1(n_N\pi^*)$ state will be expected to play an important role in the deactivation processes of PCN2NM.

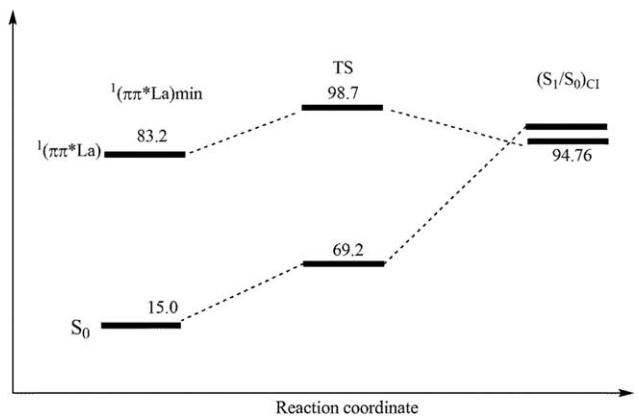

Figure 6. CASPT2 energy level diagram of pterin.

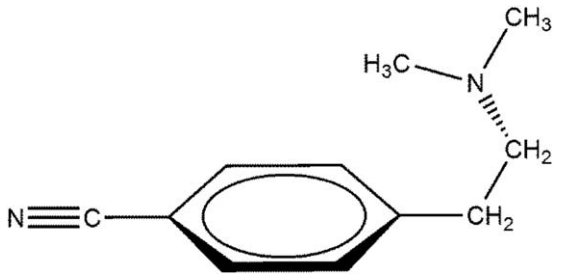

Figure 7. The schematic representation of PCN2NM.

Figure 8 summarizes the possible photophysical processes from the ground state to low-lying excited states $^1(S_1\text{-}L_b)$, $^1(S_1\text{-CT})$, $^1(S_1\text{-}L_a)$, and $^1(S_2\text{-}L_a)$ for PNM2CN. As Figure 8 shows, if the excitation energy is high enough, the molecule will be excited to S_2. Then, the molecule can relax from the Franck–Condon region of S_2 to the local minimum $^1(S_2\text{-}L_a)_{min}$. Next, the $^1(S_1\text{-}L_b)_{min}$ state will be formed through the internal conversion. A small barrier about 5.9 kcal/mol needs to be overcome from the $^1(S_1\text{-}L_b)_{min}$ state to the more stable $^1(S_1\text{-CT})_{min}$ state with an energy release of 8.4 kcal/mol. These results indicate that this photophysical process from the excitation of $S_0 \rightarrow S_2$ to formation of $^1(S_1\text{-CT})_{min}$ is favorably energetically, and the charge transfer state $^1(S_1\text{-CT})_{min}$ should be important for the strong emission band. For the alkyl-twisted conformation, the CASPT2-predicted fluorescence spectra from $^1(S_1\text{-CT})_{min}$ and $^1(S_1\text{-}L_b)_{min}$ are centered at 3.53 and 4.39 eV in the gas phase, respectively, and they are comparable to the corresponding experimental values 3.27 and 4.28 eV (see Table 2).

The possible nonradiative decay channel is also discussed here. The $^1(S_1\text{-}L_a)_{min}$ state can be obtained from the S_2 state through the conical intersection of $^1(S_2/S_1)_{CI}$. The energy differences between $^1(S_1\text{-}L_b)_{min}$ and $^1(S_1\text{-}L_a)$ are 6.0 kcal/mol for PCN2NM. Corresponding conversion from $^1(S_1\text{-}L_b)_{min}$ to $^1(S_1\text{-}L_a)_{min}$ has barrier of 6.8 kcal/mol for PCN2NM. As $^1(S_1\text{-}L_a)_{min}$ has relatively higher energy than $^1(S_1\text{-}L_b)_{min}$, it can be considered as a metastable state and will be expected to decay to the ground state through a radiationless process. Calculations reveal that there is a conical intersection between $^1(S_1\text{-}L_a)_{min}$ and S_0. The crossing point energy is slightly lower than $^1(S_1\text{-}L_a)_{min}$. As Figure 8 shows the IC decay from $^1(S_1\text{-}L_a)_{min}$ to the ground state via $^1(S_1/S_0)_{CI}$ is favorable thermodynamically because it is a nearly barrierless process. Therefore, if the

Table 2. Vertical transition and emission energies (ΔE in eV) of low-lying singlet excited states of PCN2NM.

Vertical transition energies				Vertical emission energies			
State	Transition	ΔE	f	ΔE	μ	μ_{ij}	ΔE (exp)[a]
$^1(\pi\pi^*L_b)$	$H \rightarrow L+1$	4.75	0.0042	4.39	6.00	0.27	4.28
$^1(\pi\pi^*L_a)$	$H \rightarrow L$	5.88	0.2776	2.91	6.56	1.10	
$^1(n_N\pi^*)$	$n_N \rightarrow L$	5.68	0.0276	3.53	20.22	0.93	3.27
$^1(n_N\pi^*)$	$n_N \rightarrow L+1$	6.11	0.0027				

[a] See Ref. [65].

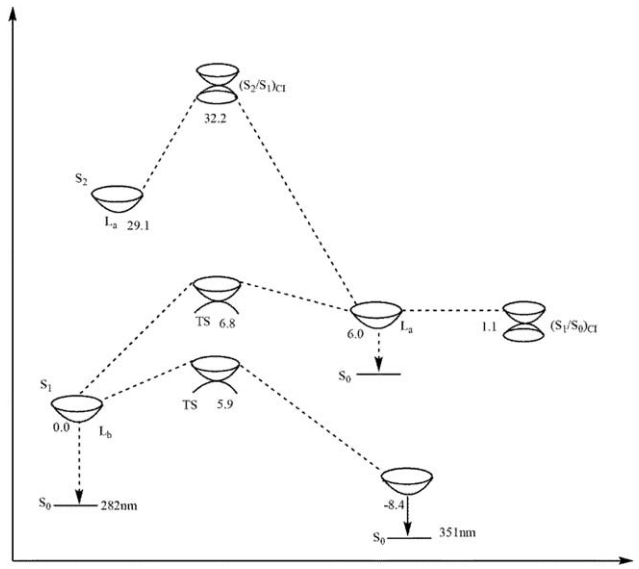

Figure 8. Relative CASPT2-energy profiles (in kcal/mol except given explicitly) for the low-lying states of PCN2NM.

PNM2CN was populated to the $^1(S_1\text{-}L_a)$ state, it could rapidly decay to the ground state with the excess energy releasing. Moreover, the IC process via $^1(S_1\text{-}L_a)_{min}$ will become important for competitive channels to the fluorescence emission.

Electronic spectra of nucleic acid bases

In recent years, the spectroscopic properties of nucleic acid bases in the gas phase and in aqueous solution have been extensively explored, both experimentally[66–74] and theoretically.[75–82] To understand the photophysical and photochemical processes in RNA and DNA, it is important to evaluate the solvent effect on excited-state properties of nucleic acid bases.

Table 3. Comparison of the vertical excitation energies of uracil.

Method	$^1(\pi\pi^*)$ (gas)	$^1(\pi\pi^*)$ (water)	$^1(n\pi^*)$ (gas)	$^1(n\pi^*)$ (water)
Present results				
TD-X3LYP/aug-cc-pvDZ+5H_2O+PCM	5.14	4.98	4.73	5.31
Previous studies				
TD-PBE0 + 4H_2O + PCM[a]	5.26	5.14	4.80	5.27
TD-B3PW91 + 9H_2O + PCM[b]	5.14	4.97	4.57	5.16
PMM/TD-B3LYP[c]	5.07	4.89	4.94	5.50
EOM-CCSDt/6–31G(d)[d]	5.89	5.96	5.31	5.75
CAM-B3LYP + 12H_2O + Ahlström[e]	5.39	5.23	5.05	5.49
RI-CC2/aug-cc-pVDZ + 6H_2O + COSMO[f]	5.40	5.21	4.94	5.50
Expt.	5.08[g]	4.77[h]	4.63[i]	5.17[g]

[a] Ref. [84]. [b] Ref. [85] [c] Ref. [77]. [d] Ref. [86]. [e] Ref. [78]. [f] Ref. [87]. [g] Ref. [88]. [h] Ref. [89]. [i] Ref. [90].

Here, we take uracil as an example to explore the methodology dependence of predicted vertical excitation energies, the absorption spectra of nucleic acid bases in the gas phase and in aqueous solution by the QM-cluster/MM and QM-cluster/polarizable continuum model (PCM) schemes combined with molecular dynamics (MD) simulations.[83]

Table 3 shows a detailed comparison of vertical transition energies of uracil by different approaches. It is noted that the TD-DFT method combined with the QM-cluster/PCM model can predict accurate absorption spectra and solvatochromic shifts, and the maximum deviation between the vertical excitation energies by TD-X3LYP/PCM and experimental values is less than 0.2 eV. This computational protocol provides an alternative way toward reliable solvent effect prediction on the low-lying states in water with relatively low computational costs.

As we can see from Figure 9 and Table 4, the QM/MM geometry optimization based on the MD equilibrated configuration can reasonably describe H-bond interactions between solute and solvent. There is a strong hydrogen bond

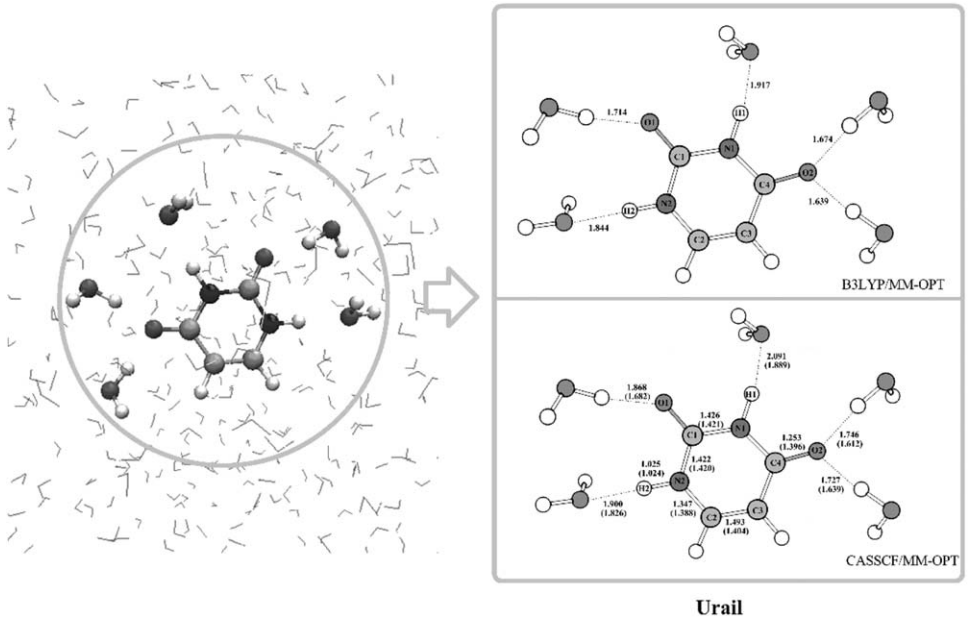

Figure 9. QM/MM-optimized structures of the ground states and first excited states of uracil.

Table 4. The vertical excitation energies and oscillator strengths of uracil in the gas phase and aqueous solution by QM-cluster/PCM.

State	ΔE (cal)	ΔE (exp)	f
Gas phase			
$S_1(n\pi^*)$	4.73	4.63[a]	0.000
$S_2(\pi\pi^*)$	5.14	5.08[b]	0.129
$S_5(\pi\pi^*)$	5.93	6.05[b]	0.031
$S_8(\pi\pi^*)$	6.42	6.63[b]	0.112
Solution phase			
$S_2(n\pi^*)$	5.31	5.17[c]	0.000
$S_1(\pi\pi^*)$	4.98	4.77[d]	0.200
$S_7(\pi\pi^*)$	6.09	6.14[d]	0.005
$S_8(\pi\pi^*)$	6.18		0.157

[a] Ref. [91]. [b] Ref. [92]. [c] Ref. [93]. [d] Ref. [94].

interaction around the uracil. Present calculations reveal that the remarkable H-bond site dependence of predicted vertical excitation energies. In particular, the H-bond around O1 site shows notable effect on the HOMO-2(π_o) $\rightarrow$ LUMO(π^*) transition with the transition energy change of 0.17 eV. The two absent H-bonds at the O2 atom site reduce the HOMO-1(n_o) $\rightarrow$ LUMO(π^*) transition energy by 0.39 eV. Moreover, all the H-bonds linking to the base in the first excited state of uracil are shorter than those in the ground state (see Fig. 9), meaning that the stronger H-bond interactions in S_1 can stabilize the first excited state, resulting in the red shifted $\pi \rightarrow \pi^*$ transition in water.

The present calculations indicate that the absorption spectra of nucleic acid bases in water strongly depend on the fluctuation of H-bond interactions in the first solvation shell of the excited states with respect to the ground state, which allow for further understanding the origin of solvent effects on the electronic spectra of nucleic acid bases in aqueous solution.

Excited-state dynamics of rare bases and analogs in the gas phase and in solution

With the rapid development of the time-resolved spectroscopy, the excited-state behaviors of nucleic acid bases and their analogs by UV light have attracted considerable attention recently. A number of the experimental studies show that all the naturally occurring nucleobases can efficiently get rid of the energy excess and quickly decay from the excited singlet states to the ground state at the subpicosecond or picosecond time scale.[95–99] Theoretically, the much effort has been devoted to identify the main reaction pathways and estimate their decay efficiency available for each bases.[100–105]

Recently, we systematically investigated the excited-state dynamics of three nucleobase related systems (see Fig. 10) using the sophisticated *ab initio* methodologies with surface hopping.[106,107] An excellent agreement is found between our theoretical calculations and the experimental findings.

Hypoxanthine. Hypoxanthine is a rare naturally occurring nucleobase analog, which was considered as a candidate with the fastest nonradiative decay among the reported natural or modified bases.[108] It has two most stable tautomers keto-N7H and keto-N9H (see Figs.10a and 10b) with small energy

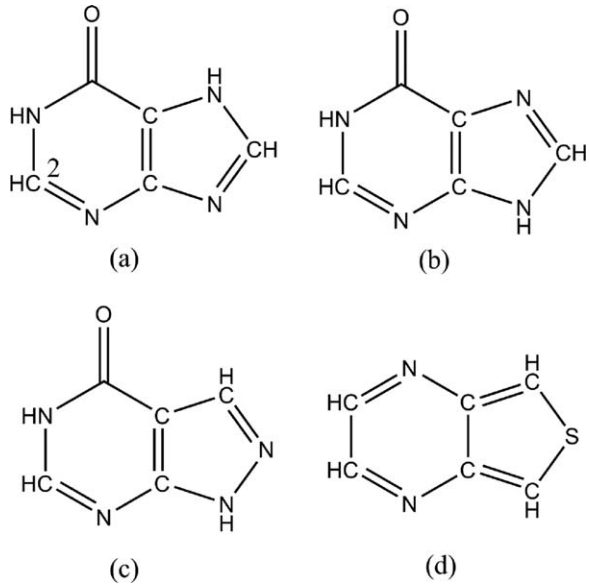

Figure 10. Structures of hypoxanthine [(a) keto-N7H; (b) keto-N9H], allopurinol [(c) keto-N9H], and thieno[3,4-b]pyrazine (d).

difference of less than 1 kcal/mol at the ground-state equilibrium geometries.[108,109] Our dynamical simulations in the gas phase demonstrate that after photoexcitation into the first bright $\pi\pi^*$ singlet state, keto-N9H exhibits a slightly faster nonadiabatic decay to the ground state than keto-N7H by about 50 fs (see Fig. 11).[106] In addition, there are four comparable reaction channels for each tautomer, all of which should be responsible for the ultrafast nonradiative decay observed experimentally.[106] These similarities imply that the two hypoxanthine tautomers may have similar decay mechanisms in the gas phase.

However, in aqueous solution, there are at least three dramatic differences between their ground-state and excited-state properties.[107] First, the distinct hydrogen bonding networks are formed between each tautomer and the surrounding water molecules. Interestingly, a π-electron hydrogen bond occurs

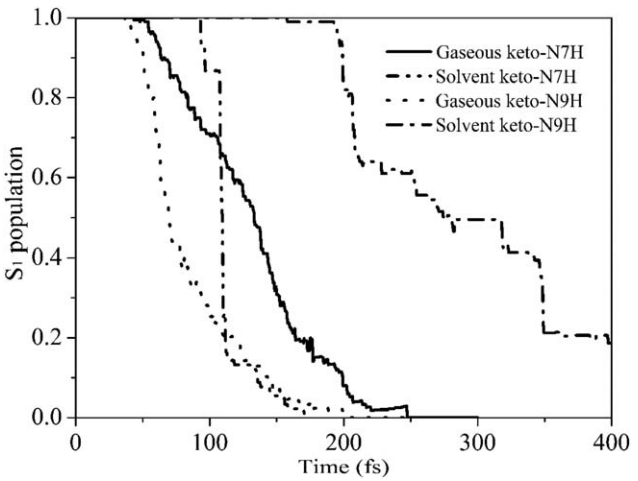

Figure 11. Time evolution of the average population of the state from respective 200 trajectories of hypoxanthine in vacuum and water.

around the N_3 site of keto-N7H, while such a phenomenon is not observed in keto-N9H. Second, keto-N7H shows a somewhat faster decay from S_1 to S_0 in water than in vacuum (112.6 vs. 137.7 fs), whereas the $S_1 \rightarrow S_0$ decay of keto-N9H becomes slower in aqueous solution (>200 fs). Third, in water environment, there is one predominant decay channel for keto-N7H, but for keto-N9H the decay channels are found to be less sensitive to the solvent effect. Such distinct photodynamical behaviors can be attributed to the aforementioned H-bond network differences around keto-N7H and keto-N9H in water environment. The presence of π-electron H-bond in the solvated keto-N7H can facilitate the $S_1 \rightarrow S_0$ nonradiative decay process.

Allopurinol. Allopurinol is a modified nucleic acid base, which is structurally similar to hypoxanthine. Fluorescence upconversion experiment showed that allopurinol riboside exhibits ultrafast excited-state relaxation in aqueous solution ($\tau < 200$ fs).[110] Our dynamics simulations indicated that allopurinol also has similar excited-state behavior with its riboside derivative.[107] In the gas phase, allopurinol keto-N9H tautomer (see Fig. 10c) has four comparable decay channels for internal conversion after evolution into the optically bright $S_1(\pi\pi^*)$ excited state. Two pathways are characterized by puckering upward at the C_2 atom, and the remaining two pathways show an inverse trend at the same position. However, only two possibilities with downward distorted conical intersection structures are found in aqueous solution. Conversely, the $S_1(\pi\pi^*)$ excited-state lifetime of allopurinol keto-N9H is predicted to be 104.7 fs in vacuum, much shorter by about 140 fs than in water. Such differences at two different environments can be ascribed to the steric interactions stepping from adjacent water molecules around the base analog. Because of the steric hindering between solute and solvent, the number of decay pathways of allopurinol keto-N9H is decreased and its excited-state lifetime is elongated.

Thieno[3,4-b]pyrazine. Thieno[3,4-b]pyrazine (TP, see Fig. 10d) is a building block for design of the narrow-bandgap organic conjugated materials,[111,112] composed of a five-membered and a six-membered rings, like hypoxanthine and allopurinol. Similarly, one main decay pathway of TP molecule can also be characterized by puckering at the C_2 atom.[9] Compared with hypoxanthine and allopurinol, the excited-state decay mechanism of TP molecule is more complicated, due to the facts that its third excited singlet state is optically bright with the strongest absorption while the first excited state is less accessible optically. After excitation into the active $S_3(\pi\pi^*)$ state, TP molecule can relax fast to the dark $S_1(n\pi^*)$ state, and then slowly evolves into its S_0 ground state. The dynamics simulations revealed that the excited TP molecule can be easily trapped in the $^1n\pi^*$ excited state, resulting in the increase of its excited-state lifetime.

Conclusions

The simulated vibronic spectra of coumarin show good agreement with the experimental bands, which allow us to reasonably interpret vibronic features in emission spectra. The excited-state properties and related photophysical processes of pterin and 2-(4-cyanophenyl)-*N*,*N*-dimethyl aminoethane (PCN2NM) have been investigated by DFT, CASSCF, and CASPT2 calculations, and possible radiationless decay pathways have been also explored based on the search of conical intersection points. The spectroscopic properties of key nucleic acid bases in water have been studied by the combined QM/MM and cluster-continuum computational protocol, and the hydrogen bond network can remarkably modify their absorption spectra. The excited-state nonadiabatic decay of biologically relevant hypoxanthine and allopurinol has been explored using *ab initio* surface-hopping dynamics simulations in the gas phase and in aqueous solution. The present QM/MM simulations with surface hopping show that the hydrogen bonding networks and the solvent steric hindering can modify their photodynamical behaviors remarkably.

Keywords: excited states · vibronic spectra · ultrafast nonradiative decay · photodynamics · solvent effect

How to cite this article: J. Li, X. Guo, Y. Zhao, Z. Cao. *Int. J. Quantum Chem.* **2015**, *115*, 680–688. DOI: 10.1002/qua.24879

[1] F. Negri, G. Orlandi, In Theoretical and Computational Chemistry, Vol. *16*; M. Olivucci, Ed.; Elsevier, **2005**; pp. 129–169.
[2] M. Dierksen, S. Grimme, *J. Chem. Phys.* **2004**, *120*, 3544.
[3] R. Improta, V. Barone, F. Santoro, *J. Phys. Chem. B* **2007**, *111*, 14080.
[4] F. Santoro, A. Lami, R. Improta, V. Barone, *J. Chem. Phys.* **2007**, *126*, 184102.
[5] F. Santoro, A. Lami, R. Improta, J. Bloino, V. Barone, *J. Chem. Phys.* **2008**, *128*, 224311.
[6] F. Santoro, V. Barone, *Int. J. Quantum Chem.* **2010**, *110*, 476.
[7] V. Barone, J. Bloino, M. Biczysko, F. Santoro, *J. Chem. Theory Comput.* **2009**, *5*, 540.
[8] J. Bloino, M. Biczysko, F. Santoro, V. Barone, *J. Chem. Theory Comput.* **2010**, *6*, 1256.
[9] J. Tatchen, C. M. Marian, *Phys. Chem. Chem. Phys.* **2006**, *8*, 2133.
[10] R. Improta, V. Barone, F. Santoro, *Angew. Chem. Int. Ed.* **2007**, *46*, 405.
[11] M. Biczyskoa, J. Bloinoa, V. Barone, *Chem. Phys. Lett.* **2009**, *471*, 143.
[12] S. Salzmann, C. M. Marian, *Photochem. Photobiol. Sci.* **2009**, *8*, 1655.
[13] B. Klaumünzer, D. Kröner, P. Saalfrank, *J. Phys. Chem. B* **2010**, *114*, 10826.
[14] J. P. Carrasco, M. Fanuel, A. C. Eddin, D. Jacquemin, *Chem. Phys. Lett.* **2013**, *556*, 122.
[15] J. Li, Z. Rinkevicius, Z. Cao, *J. Chem. Phys.* **2014**, *141*, 014306.
[16] M. Olivucci, A. Sinicropi, In Theoretical and Computational Chemistry, Vol. *16*; M. Olivucci, Ed.; Elsevier, **2005**; pp. 1–33.
[17] F. Bernardi, M. Olivucci, M. A. Robb, *Chem. Soc. Rev.* **1996**, *25*, 321.
[18] X. Chen, X. Xu, Z. Cao, *J. Phys. Chem. A* **2007**, *111*, 9255.
[19] X. Chen, Y. Zhao, Z. Cao, *J. Chem. Phys.* **2009**, *130*, 144307.
[20] M. J. Bearpark, M. A. Robb, H. B. Schlegel, *Chem. Phys. Lett.* **1994**, *223*, 269.
[21] A. H. Zewail, *Angew. Chem. Int. Ed.* **2000**, *39*, 2586.
[22] X. Guo, Z. Cao, *J. Chem. Phys.* **2012**, *137*, 224313.
[23] X. Guo, Z. Lan, Z. Cao, *Phys. Chem. Chem. Phys.* **2013**, *15*, 10777.
[24] O. Christiansen, H. Koch, P. Jorgensen, *Chem. Phys. Lett.* **1995**, *243*, 409.
[25] A. B. Trofimov, J. Schirmer, *J. Phys. Chem. B* **1995**, *28*, 2299.
[26] J. F. Stanton, R. J. Bartlett, *J. Chem. Phys.* **1993**, *98*, 7029.
[27] M. W. Schmidt, M. S. Gordon, *Annu. Rev. Phys. Chem.* **1998**, *49*, 233.
[28] R. J. Buenker, S. D. Peyerimhoff, W. Butscher, *Mol. Phys.* **1978**, *35*, 771.
[29] H.-J. Werner, P. J. Knowles, *J. Chem. Phys.* **1988**, *89*, 5803.

[30] J. Finley, P. Å. Malmqvist, B. O. Roos, L. Serrano-Andrés, *Chem. Phys. Lett.* **1998**, *288*, 299.
[31] H. Lischka, M. Dallos, R. Shepard, *Mol. Phys.* **2002**, *100*, 1647.
[32] B. H. Lengsfield, P. Saxe, D. R. Yarkony, *J. Chem. Phys.* **1984**, *81*, 4549.
[33] P. Celani, H.-J. Werner, *J. Chem. Phys.* **2003**, *119*, 5044.
[34] H. Lischka, M. Dallos, P. G. Szalay, D. R. Yarkony, R. Shepard, *J. Chem. Phys.* **2004**, *120*, 7322.
[35] R. Bauernschmitt, R. Ahlrichs, *Chem. Phys. Lett.* **1996**, *256*, 454.
[36] I. Frank, J. Hutter, D. Marx, M. Parrinello, *J. Chem. Phys.* **1998**, *108*, 4060.
[37] M. Filatov, S. Shaik, *Chem. Phys. Lett.* **1999**, *304*, 429.
[38] M. Elstner, *Theor. Chem. Acc.* **2006**, *116*, 316.
[39] F. Furche, R. Ahlrichs, *J. Chem. Phys.* **2002**, *117*, 7433.
[40] I. Tavernelli, B. F. E. Curchod, U. Rothlisberger, *J. Chem. Phys.* **2009**, *131*, 196101.
[41] A. Becke, *J. Chem. Phys.* **1993**, *98*, 5648.
[42] C. Adamo, V. Barone, *J. Chem. Phys.* **1999**, *110*, 6158.
[43] A. Dreuw, M. Head-Gordon, *Chem. Rev.* **2005**, *105*, 4009.
[44] R. Improta, G. Scalmani, M. J. Frisch, V. Barone, *J. Chem. Phys.* **2007**, *127*, 074504.
[45] F. Santoro, A. Lami, R. Improta, V. Barone, *J. Chem. Phys.* **2007**, *126*, 184102.
[46] F. Duschinsky, *Acta Phisicochim. USSR* **1937**, *7*, 551.
[47] M. Ben-Nun, J. Quenneville, T. J. Martinez. *J. Phys. Chem. A* **2000**, *104*, 5161.
[48] M. Santer, U. Manthe, G. Stock, *J. Chem. Phys.* **2001**, *114*, 2001.
[49] J. C. Tully, *J. Chem. Phys.* **1990**, *93*, 1061.
[50] M. Barbatti, R. Shepard, H. Lischka, In Conical Intersections: Theory, Computation and Experiment, Advanced Series in Physical Chemistry, Vol. *17*; W. Domcke, D. R. Yarkony, H. Köppel, Eds.; World Scientific: Singapore, **2011**; pp. 415–462.
[51] A. Warshel, M. Levitt, *J. Mol. Biol.* **1976**, *103*, 227.
[52] R. A. Friesner, V. Guallar, *Annu. Rev. Phys. Chem.* **2005**, *56*, 389.
[53] W. L. Jorgensen, J. Chandrasekhar, J. D. Madura, R. W. Impey, M. L. Klein, *J. Chem. Phys.* **1983**, *79*, 926.
[54] U. S. Raikar, C. G. Renuka, Y. F. Nadaf, B. G. Mulimani, *J. Mol. Struct.* **2006**, *787*, 127.
[55] R. Paula, A. E. Machado, J. A. de Miranda, *J. Photochem. Photobiol. A* **2004**, *165*, 109.
[56] Y. Kashman, K. R. Gustafson, R. W. Fuller, J. H. Cardellina, J. B. McMahon, M. J. Currens, R. W. Buckheit, S. H. Hughes, G. M. Cragg, M. R. Boyd, *J. Med. Chem.* **1992**, *35*, 2735.
[57] W. W. Mantulin, P. S. Song, *J. Am. Chem. Soc.* **1973**, *95*, 5122.
[58] A. W. Schüttelkopf, L. W. Hardy, S. M. Beverley, W. N. Hunter, *J. Mol. Biol.* **2005**, *352*, 105.
[59] J. M. Hevel, M. A. Marletta, *Biochemistry* **1992**, *31*, 7160.
[60] W. Pfleiderer, In Chemistry and Biology of Pteridines and Folates, J. E. Ayling, M. G. Nair, C. M. Baugh, Eds.; Plenum Press: New York, **1993**, pp. 1–16.
[61] H. Tiemeier, D. Fekkes, A. Hofman, R. H. van Tuijl, A. J. Kiliaan, M. M. B. Breteler, *Psychiatry Res.* **2006**, *145*, 199.
[62] C. Lorente, A. H. Thhomas, *Acc. Chem. Res.* **2006**, *39*, 396.
[63] Z. R. Grabowski, K. Rotkiewicz, W. Rettig, *Chem. Rev.* **2003**, *103*, 3899.
[64] M. Van der Auweraer, L. Viaene, P. Van Haver, F. C. De Schryver, *J. Phys. Chem.* **1993**, *97*, 7178.
[65] M. Van der Auweraer, L. Viaene, P. Van Haver, F. C. De Schryver, *J. Phys. Chem.* **1993**, *97*, 7178.
[66] M. Fujii, T. Tamura, N. Mikami, M. Ito, *Chem. Phys. Lett.* **1986**, *126*, 583.
[67] M. A. Morsy, A. M. Al-Somali, A. Suwaiyan, *J. Phys. Chem. B* **1999**, *103*, 11205.
[68] E. Nir, L. Grace, B. Brauer, M. S. de Vries, *J. Am. Chem. Soc.* **1999**, *121*, 4896.
[69] E. Nir, C. Janzen, P. Imhof, K. Kleinermanns, M. S. de Vries, *J. Chem. Phys.* **2001**, *115*, 4604.
[70] E. Nir, C. Janzen, P. Imhof, K. Kleinermanns, M. S. de Vries, *Phys. Chem. Chem. Phys.* **2002**, *4*, 732.
[71] F. Piuzzi, M. Mons, I. Dimicoli, B. Tardivel, Q. Zhao, *Chem. Phys.* **2001**, *270*, 205.
[72] M. Y. Choi, R. E. Miller, *J. Am. Chem. Soc.* **2006**, *128*, 7320.
[73] A. O. Alyoubi, R. H. Hilal, *Biophys. Chem.* **1995**, *55*, 231.
[74] C. E. Crespo-Hernandez, B. Cohen, P. M. Hare, B. Kohler, *Chem. Rev* **2004**, *104*, 1977.
[75] J. Lorentzon, M. P. Fuelscher, B. O. Roos, *J. Am. Chem. Soc.* **1995**, *117*, 9265.
[76] M. P. Fulscher, L. Serrano-Andres, B. O. Roos, *J. Am. Chem. Soc.* **1997**, *119*, 6168.
[77] C. Zazza, A. Amadei, N. Sanna, A. Grandi, G. Chillemi, A. D. Nola, M. D. Abramo, M. Aschi, *Phys. Chem. Chem. Phys.* **2006**, *8*, 1385.
[78] J. C. Olsen, K. Aidas, K. V. Mikkelsen, J. Kongsted, *J. Chem. Theory Comput.* **2010**, *6*, 249.
[79] S. Perun, A. L. Sobolewski, W. Domcke, *J. Am. Chem. Soc.* **2005**, *127*, 6257.
[80] A. Broo, A. Holm, *J. Phys. Chem. A* **1997**, *101*, 3589.
[81] M. K. Shukla, J. Leszczynski, *J. Comput. Chem.* **2004**, *25*, 768.
[82] H. Chen, S. Li, *J. Phys. Chem. A* **2006**, *110*, 12360.
[83] Y. Zhao, Z. Cao, *J. Theor. Comput. Chem.* **2013**, *12*, 1341013.
[84] T. Gustavsson, A. Bànyàsz, E. Lazzarotto, D. Markovitsi, G. Scalmani, M. J. Frisch, V. Barone, R. Improta, *J. Am. Chem. Soc.* **2006**, *128*, 607.
[85] V. Ludwig, K. Coutinho, S. Canuto, *Phys. Chem. Chem. Phys.* **2007**, *9*, 4907.
[86] E. Epifanovsky, K. Kowalski, P. D. Fan, M. Valiev, S. Matsika, A. I. Krylov, *J. Phys. Chem. A* **2008**, *112*, 9983.
[87] M. Etinski, C. M. Marian, *Phys. Chem. Chem. Phys.* **2010**, *12*, 4915.
[88] L. B. Clark, G. G. Peschel, I. Tinoco, *J. Phys. Chem.* **1965**, *69*, 3615.
[89] W. A. Eaton, T. P. Lewis, *J. Chem. Phys.* **1970**, *53*, 2164.
[90] C. A. Sprecher, W. C. Johnson, *Biopolymers* **1977**, *16*, 2243.
[91] W. A. Eaton, T. P. Lewis, *J. Chem. Phys.* **1970**, *53*, 2164.
[92] L. B. Clark, G. G. Peschel, I. Tinoco, *J. Phys. Chem.* **1965**, *69*, 3615.
[93] C. A. Sprecher, W. C. Johnson, *Biopolymers* **1977**, *16*, 2243.
[94] D. Voet, W. B. Cratzer, R. A. Cox, P. Doty, *Biopolymers* **1963**, *1*, 193.
[95] S. Ullrich, T. Schultz, M. Z. Zgierski, A. Stolow, *J. Am. Chem. Soc.* **2004**, *126*, 2262.
[96] C. Canuel, M. Mons, F. Piuzzi, B. Tardivel, I. Dimicoli, M. Elhanine, *J. Chem. Phys* **2005**, *122*, 074316.
[97] S. Ullrich, T. Schultz, M. Z. Zgierski, A. Stolow, *J. Am. Chem. Phys.* **2004**, *126*, 2262.
[98] H. Kang, K. T. Lee, B. Jung, Y. J. Ko, S. K. Kim, *J. Am. Chem. Soc.* **2002**, *124*, 12958.
[99] H. Satzger, D. Townsend, M. Z. Zgierski, S. Patchkovskii, S. Ullrich, A. Stolow, *Proc. Natl. Acad. Sci. USA* **2006**, *103*, 10196.
[100] M. Barbatti, A. J. A. Aquino, J. J. Szymczak, D. Nachtigallová, P. Hobza, H. Lischka, *Proc. Natl. Acad. Sci. USA* **2010**, *107*, 21453.
[101] M. Barbatti, H. Lischka, *J. Am. Chem. Phys.* **2008**, *130*, 6831.
[102] M. Barbatti, J. J. Szymczak, A. J. A. Aquino, D. Nachtigallová, H. Lischka, *J. Chem. Phys.* **2011**, *134*, 014304.
[103] M. Barbatti, A. J. A. Aquino, J. J. Szymczak, D. Nachtigallová, H. Lischka, *Phys. Chem. Chem. Phys.* **2011**, *13*, 6145.
[104] Z. Lan, E. Fabiano, W. Thiel, *Chem. Phys. Chem.* **2009**, *10*, 1225.
[105] Z. Lan, E. Fabiano, W. Thiel, *J. Phys. Chem. B* **2009**, *113*, 3548.
[106] X. Guo, Y. Zhao, Z. Cao, *Phys. Chem. Chem. Phys.* **2014**, *16*, 15381.
[107] X. Guo, Y. Zhao, Z. Cao, *J. Phys. Chem. A* **2014**, *118*, 9013.
[108] J. Chen, B. Kohler, *Phys. Chem. Chem. Phys.* **2012**, *14*, 10677.
[109] B. Hernández, F. J. Luque, M. Orozco, *J. Org. Chem.* **1996**, *61*, 5964.
[110] J. P. Villabona-Monsalve, R. E. Islas, W. Rodríguez-Córdoba, S. Matsika, J. Peón, *J. Phys. Chem. A* **2013**, *117*, 898.
[111] L. Cuff, M. Kertesz, *J. Chem. Phys.* **1997**, *106*, 5541.
[112] O. Kwon, M. L. McKee, *J. Phys. Chem. A* **2000**, *104*, 7106.

Revised: 10 December 2014
Received: 28 September 2014
Accepted: 7 January 2015
Published online 13 February 2015